The Influence of the Visco-Elastic Properties of Covering Materials on the Rolling Process of Two Cylinders

Scheuter, Karl R.; Pfeiffer, Günter

(1969)

THE INFLUENCE OF THE VISCO-ELASTIC PROPERTIES OF COVERING MATERIALS ON THE ROLLING PROCESS OF TWO CYLINDERS

Karl R. Scheuter and Günter Pfeiffer*

Abstract: The stress strain behaviour of visco-elastic materials has been investigated. A special measuring device was used to characterize the visco-elastic properties of cylinder coverings. The data for some typical covering materials used for inking and pressure rollers will be discussed.

A theoretical analysis of the stress and strain in the nip will be presented as a function of the visco-elastic properties of the materials. The results will be compared to measurements of the vertical and tangential forces developed between a hard roller and an inking roller and the pressure distribution in the nip.

1. General Observations About The Rolling Process

Rollers which roll on one another are essentially construction features of every printing press. It is characteristic for every one of these roller combinations that at least one roller is covered with a comparatively soft cover. The composition of the roller covers used varies greatly. Commonly used today are synthetic and

* Institute for Printing Machines and Printing Processes of the Technical University Darmstadt

rubber covers of all degrees of hardness, covers made of rubber with vulcanized tissue as well as covers consisting of several paper layers.

The tasks fulfilled by the rolling processes in the printing press may be divided into three main groups.

1. The printing process in which the ink relief of the printing form is transferred to the material to be printed on.

2. The rolling processes of the ink rollers, dampening rollers and form rollers.

3. The reeling and re-reeling processes of the paper web which also must be considered a rolling process.

All these rolling processes were subjects of many separate printing research experiments, in which special influences were individually examined. If we on the other hand, try to depict the common factors of these rolling systems, we arrive at a rolling system that consists of two rigid rollers, of which one is covered with a comparatively soft cover.

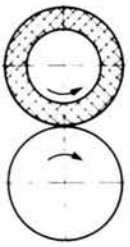

setting of the rollers
force acting between the rollers
pressure distribution in the nip
the nip width
tangential force
tangential force distribution in the nip
slip between the rollers

Illustration 1: Elementary Rolling System

Illustration 1 shows an elementary rolling system and all influence factors of interest that have to be determined in their dependency on the geometry, the cover material, the rate of revolutions and the temperature. Although this simple rolling system neglects all significant factors in printing techniques--the rollers are smooth and dry-- no exact mathematical theories exist

which makes the computation of the above mentioned values possible.

If two rollers are pressed against each other, it becomes evident that deformations take place only in the cover material. Therefore, the determination of the characteristics of the cover material is a prerequisite for any computation. Anyone faced with the task of computing the bending of a beam quickly learns, that he must know the elasticity modulus of the beam material and that with the same geometry of the beam, the bending is solely dependent on this value. In the pertinent literature on rolling tests, on the other hand, the elasticity modulus is rarely listed. Usually, only the Shore-hardness is mentioned which, however, does not suffice as a characteristic quantity for the cover material. The elasticity modulus is an essential prerequisite in the study of the rolling process. Unfortunately, contrary to metallic working materials, this is not a constant for the cover materials used in printing presses. Instead, it is to a great extent dependent on temperature and stress time.

2. Characterization of the Visco-Elastic Behaviour of Roller Covers

Rubber and rubber-like synthetic materials were termed visco-elastic due to their behaviour during mechanical stress. In order to clarify visco-elastic behaviour, models made of springs and dampers are used.

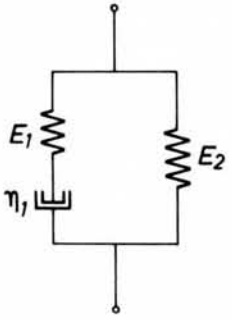

$\eta_1 = viscosity$

$\tau_1 = \frac{\eta_1}{E_2}$ *relaxation time*

$\Delta\sigma_t = \Delta\varepsilon \cdot E_1 \cdot e^{-\frac{t}{\tau_1}} + \Delta\varepsilon \cdot E_2$

$\frac{\Delta\sigma_t}{\Delta\varepsilon} = E_{(t)} = E_1 \cdot e^{-\frac{t}{\tau}} + E_2$

Ill. 2: Model of a visco-elastic body

The model in Illustration 2 shows the simplest form of a visco-elastic body. Therein the springs characterize the purely elastic behaviour such as it exists in metallic materials. The dampers represent the purely viscous behaviour which corresponds to the viscosity of liquids. If this model is deformed, the time dependency of the force is solely caused by the dampers. The temperature dependency of this force must also be solely related to the change of the viscosity of the damper. A deformation of this model at the time t=0 by $\Delta\varepsilon$ results in a stress $\Delta\sigma_t$ which at constant strain gradually becomes smaller. This shows that the E-modulus must also be a value dependent on time.

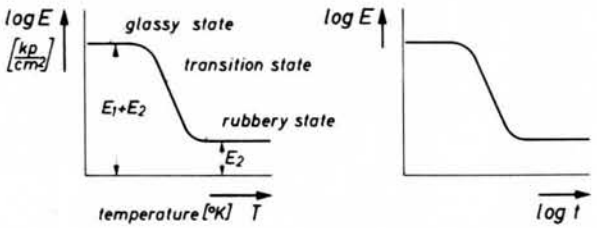

Ill. 3: The dependency of the Elasticity Modulus on temperature and strain time.

In Illustration 3 the dependency of the E-modulus--as existing in the model of Illustration 2--on temperature and time is shown. At very low temperatures, in glassy state, the viscosity of the damper becomes extremely great and the E-modulus is only determined by the springs E_1 and E_2. In the transition zone the viscosity of the damper becomes effective and the E-modulus is lowered with increasing temperature. In the rubber-elastic area the viscosity of the damper is almost non-existent and the E-modulus is only determined by E_2. A similar curve of the E-modulus also results from the deformation time. If the damper is compressed very quickly, very great forces have to be overcome and a high

E-modulus becomes effective. On the other hand, in very slow deformation the resistance of the damper is very low.

A real visco-elastic body is naturally, not as simple in construction as this working model. However, its behaviour may in principle be demonstrated very well by it. The area of application of our cover materials lies in the rubber-elastic range and at the beginning of the transition zone.

From all that was said so far, we are faced with the task of determining the E-modulus of cover materials in dependency on temperature and on the deformation frequency. If a rubber sample is subjected to a sinusoidally changing deformation, the force required for this deformation is likewise changed sinusoidally. However, between the maximum of the deformation and the maximum of the force, there occurs a time shifting by the phase angle δ.

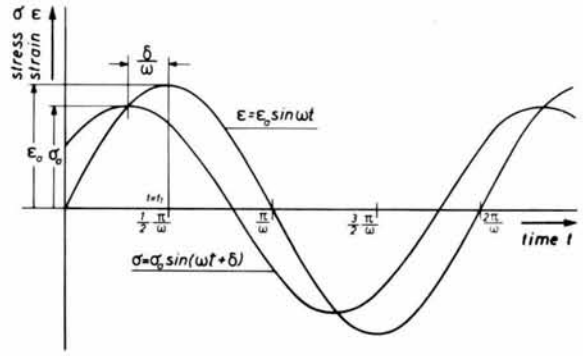

Ill. 4: Stress and strain as a function of time

Illustration 4 shows the stress and strain during sinusoidal deformation in its time curve. At the time t_1 the strain has reached its maximum value, the stress, however, has reached its maximum some time before. With a metallic working material both maxima would coincide.

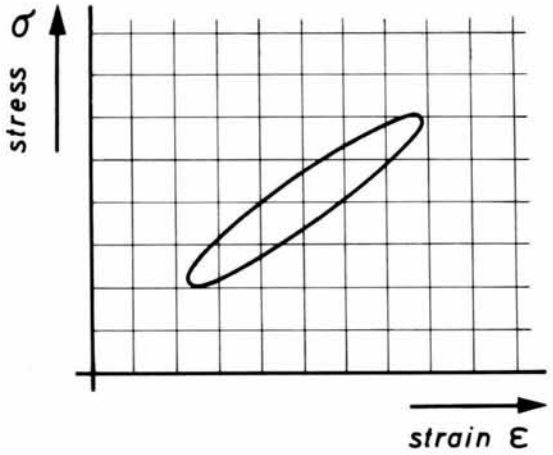

Ill.: 5: Force-and-Displacement Diagram: Damping Ellipse

The effects of the visco-elastic behaviour are most evident in the stress and strain diagram (Illustration 5). During a deformation cycle a part of the energy which is required for the deformation process is not regained during the relaxation process but instead converted into heat. The area of the damping ellipse is a measure for this loss energy. The greater the phase angle δ, the greater is the loss increment.

Some difficulties arise in defining the E-modulus. We saw that the strain

$$\varepsilon = \varepsilon_a \sin \omega t$$

is generated by the stress

$$\sigma = \sigma_a \sin (\omega t + \delta)$$

If the stress is analyzed as a part that runs in phase with the deformation and which is required for the overcoming of the purely elastic resistance, then a dynamic E-modulus, also termed storage modulus

$$E' = \frac{\sigma_a}{\varepsilon_a} \cos\delta$$

may be defined.

That portion of the stress which runs in phase with the deformation speed and which is required for the overcoming of purely viscous resistance

$$E'' = \frac{\sigma_a}{\varepsilon_a} \sin\delta$$

is defined as loss modulus.

The mode of operation of these two moduli may be represented by a vector diagram.

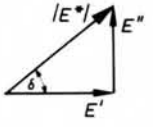

E' and E'' may be joined vectorially to form the complex E-modulus. The following is valid for the absolute value of the complex E-modulus.

$$E^* = \frac{\sigma_a}{\varepsilon_a}$$

and the relationship

$$\frac{E''}{E'} = \tan\delta = d$$

is designated loss factor.

3. Test Equipment for the Determination of the Visco-Elastic Properties of Roller Covers.

A test unit for the determination of the visco-elastic properties (complex E-modulus, storage modulus, loss modulus, loss factor) of cover materials was developed at the Institute. The mode of operation of this equipment is drawn schematically in Illustration 6.

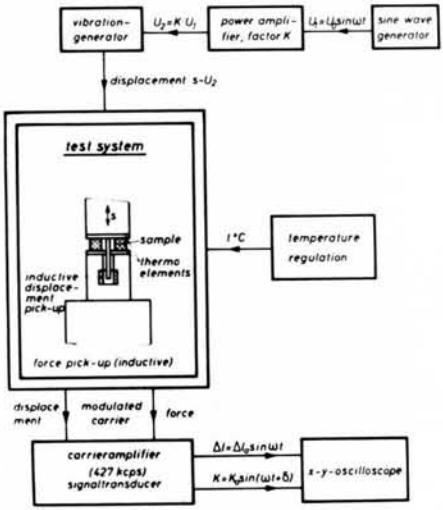

Ill. 6: Schematic representation of the Measuring Apparatus for the determination of the visco-elastic properties of cover materials

In this unit rubber samples of 10 mm length and 10 mm diameter are subjected to a chronological sinusoidally altering change in pressure deformation. A vibrator which is controlled via a power amplifier by a sine generator with frequencies from 1 Hz to 200 Hz is used for the production of this change in pressure deformation.

The deformation of the rubber sample through the impact rod of the vibrator as well as the force required for the deformation are determined by means of an inductive force-and-displacement measuring system and are made visual on an oscilloscope in a force-and-displacement graph. The visco-elastic characteristic values may be determined by the thus created damping ellipse.

4. The Visco-Elastic Data of Pressure and Ink Roller Covers.

The complex E-modulus and loss factor for several pressure and ink roller covers was determined in dependency on the temperature and

the deformation frequency.

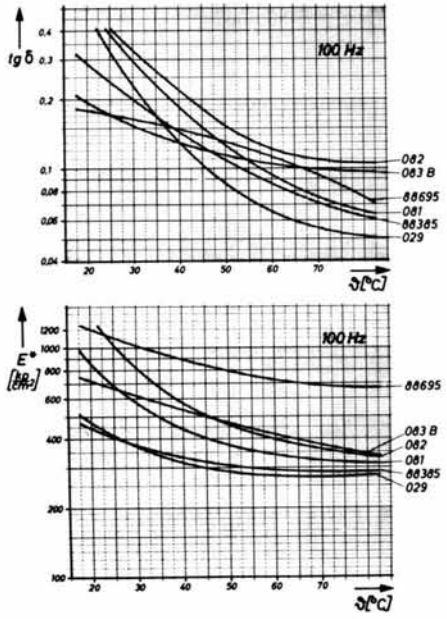

Ill. 7: The complex E-modulus and loss factor of pressure roller covers as function of the temperature.

Illustration 7 shows measuring data derived from pressure roller materials at temperatures between 20 and 80 degrees C with a deformation frequency of 100 cps. All covers have a decrease of the E-modulus at increasing temperature in common; the type of decrease, however, varies. The loss factor also decreases with increasing temperature. Even without knowing details about the effects of these values on the rolling process, a comparative evaluation of the covers may be made. If we start with the assumption that for satisfactory printing results a certain compressive stress is required, a pressure roller material which at the same E-modulus has the lowest loss factor, will heat up the least. Material 029 will, therefore, be better than material 88385. Furthermore, we recognize that the heating up of a pressure roller does not merely stop

at a certain ignition temperature because the produced heat and the carried off heat coincide, instead we find that at higher temperatures less heat is evidently produced, since the loss factor has become smaller. The material properties are thus more favourable in heated condition than in cold.

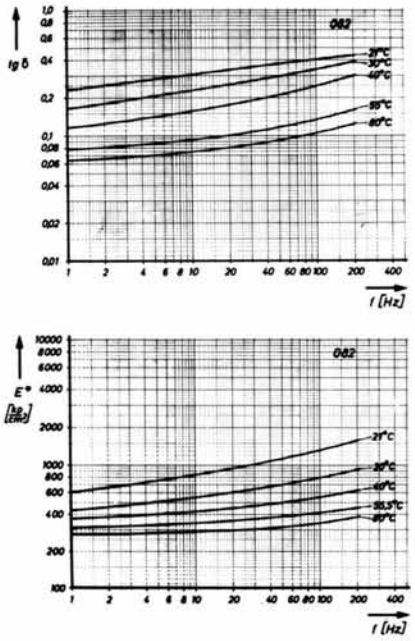

Ill. 8: The complex E-modulus and loss factor of a pressure roller cover in dependency on the deformation frequency.

In Illustration 8 the complex E-modulus and the loss factor were reproduced in dependency on the deformation frequency. With all materials examined, the E-modulus and the loss factor increased with rising frequency. As a result of this behaviour, any change of printing speed is interrelated with a change in the cover material properties.

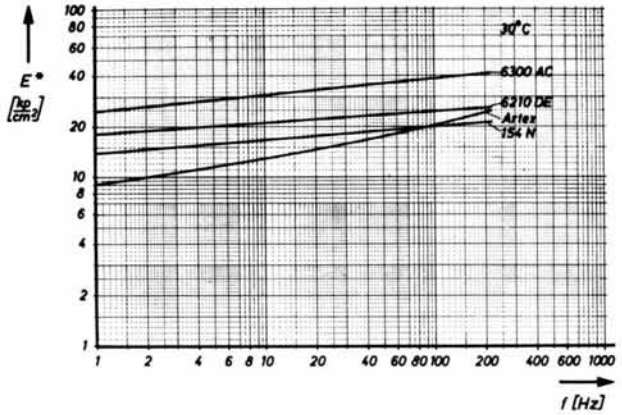

Ill. 9: Complex E-modulus for Ink Roller Covers in Dependency on the Deformation Frequency.

In Illustration 9 the E-modulus was shown as dependent on the deformation frequency at constant temperature. The E-modulus increases with increased deformation frequency. In the double logarithmic graph used here, the frequency dependency of the E-modulus shows an approximately linear course, at least the curves may with sufficient accuracy be substituted by straight lines in a certain frequency range. The dependency of the E-modulus on the frequency may accordingly be defined by the power function

$$E^*_{(f)} = E^*_1 \left(\frac{f}{f_1}\right)^y$$

The power factor y is determined by the slope of the straight line in the double logarithmic paper. E_1^* corresponds to the E-modulus that was measured at the frequency f_1.

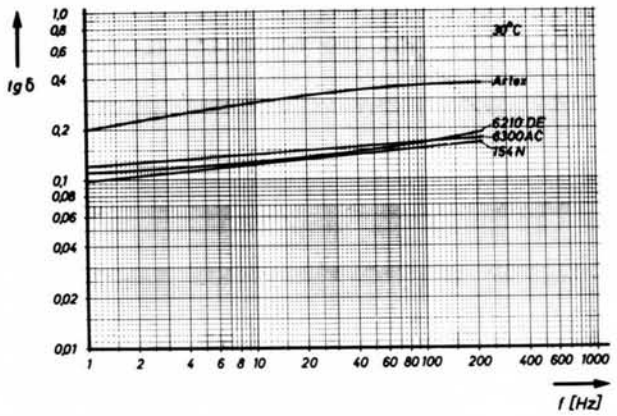

Ill. 10: Loss factor of ink roller covers in dependency on deformation frequency.

In Illustration 10 the loss factor of the ink roller covers shown in illustration 9, is reproduced. The loss factor lies between o.1 and 0.4. With increasing frequency the loss factor increases. Three cover materials have approximately similar loss factors; the cover material Artex, however, clearly deviates from this. If the dependency of the loss factor on the deformation frequency results in a straight line in the double logarithmic graph, then the loss factor may also be described by a power function.

5. Theoretical Considerations About The Influence of the Visco.Elastic Properties on the Rolling Process of Two Rollers.

After characterizing the visco-elastic properties of roller covers and after demonstrating a test unit to determine them experimentally, we will now try to determine the influence of the visco-elastic behaviour on the rolling process.

Emphasizing the aspect of rolling friction similar problems were studied by several authors.

In order to determine the rolling moment

required to maintain the rotary motions, Funk (1938) refers to the properties of the cover material. In his dissertation published in 1938, he already recognized that the rolling friction has to be attributed solely to the viscous losses in the cover materials. Funk considered the effects of visco-elastic behaviour of the cover material on the pressure distribution, however, was unable to clearly recognize and define the visco-elastic properties.

Independently of Funk, Tabor (1952/1955) and Evans (1954) arrived at the same conclusion, namely that the rolling friction is caused by the visco-elastic losses in bodies rolling upon each other.

Flom (1961) discussed the dependency of the visco-elastic properties on temperature and on the deformation speed and showed that the rolling friction changes accordingly.

May, Morris and Atack (1951) computed the rolling friction with the aid of a model composed of springs and dampers. The visco-elastic behaviour is characterized by a Maxwell-element made of springs and dampers and a spring connected parallely thereto. Hunter (1961) and Moreland (1962/1967) dealt with rolling friction by assuming a relaxation time spectrum of a visco-elastic material. Their theoretical considerations presuppose that no tangential forces are effective in the nip.

The following theoretical considerations are based on an elastic model working material. The visco-elastic properties obtained by experiment are then substituted in the equation for the elements of the visco-elastic model and thus enable us to arrive at a simple analysis of the influence of the cover material properties on the rolling process.

Starting point for these considerations is the rolling process between two purely elastic metal rollers. As long as no large tangential forces are transferred, the pressure distribution in the nip is symmetrical to the connecting line of both

roller centers. If we observe an element of the surface while passing the zone of pressure, we note that the deformation of this element occurs chronologically viewed symmetrically. At the time t = 0 deformation starts, at $t = t_a$ it reaches its maximum and at the time $t = 2\,t_a$ returns to zero. In illustration 11 the chronological curve of the deformation of a surface element was depicted.

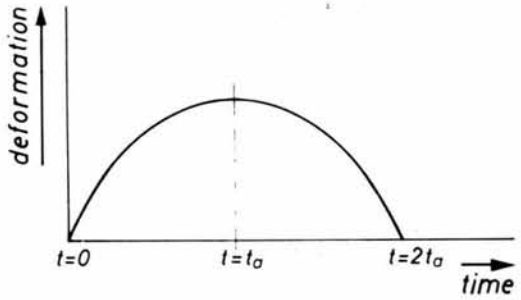

Ill. 11: Chronological curve of the deformation of a surface element while passing the nip.

In order to be able to describe the time dependency of this deformation simply mathematically, we substitute for the unknown deformation curve in first approximation a chronologically sinusoidally changing strain

$$\varepsilon_{\omega t} = \varepsilon_a \sin \omega t \qquad (1)$$

with ε_a amplitude of deformation and $2\omega t_a = \pi$ the half cycle of a sine wave.

For metallic working materials we hereby get immediately the stress

$$\sigma = E\,\varepsilon = E\varepsilon_a \sin\omega t$$

which also runs symmetrically.

In a visco-elastic material, the symmetrical deformation curve will not elicit a symmetrical stress distribution because of the time dependency

of this process. The actual stress distribution first shall be analyzed by means of a working model. For this purpose the same visco-elastic model is used that was already used in illustration 2. A small strain of this model results in a small stress decreasing with time.

$$\Delta \sigma_t = \Delta \varepsilon E_1 e^{-\frac{t}{\tau}} + \Delta \varepsilon E_2 \qquad (2)$$

If the strain changes continuously, then due to the superposition of the stresses elicited by the single strain steps, there results for the total stress active at the time t

$$\sigma_t = E_1 e^{-\frac{t}{\tau}} \int_{t_i=0}^{t_i=t} \frac{d\varepsilon}{dt} e^{\frac{t_i}{\tau}} dt + E_2 \varepsilon_t \qquad (3)$$

if the deformation results sinusoidally, we get from (1)

$$\frac{d\varepsilon}{dt} = \varepsilon_a \omega \cos \omega t \qquad (4)$$

and for the stress as function of t the following is valid

$$\sigma_{\omega t} = E_1 \varepsilon_a e^{-\frac{t}{\tau}} \int_0^t \omega \cos \omega t \, e^{\frac{t}{\tau}} dt + E_2 \varepsilon_a \sin \omega t \qquad (5)$$

After the integration we get

$$\sigma_{\omega t} = E_1 \varepsilon_a e^{-\frac{t}{\tau}} \Bigg|_0^t e^{\frac{t}{\tau}} \frac{\frac{\omega}{\tau} \cos \omega t + \omega^2 \sin \omega t}{\tau^{-2} + \omega^2} + E_2 \varepsilon_a \sin \omega t$$

$$\sigma_{\omega t} = E_1 \varepsilon_a e^{-\frac{t}{\tau}} \left[\frac{e^{\frac{t}{\tau}} \left(\frac{\omega}{\tau} \cos \omega t + \omega^2 \sin \omega t \right) - \frac{\omega}{\tau}}{\tau^{-2} + \omega^2} \right] + E_2 \varepsilon_a \sin \omega t$$

If this equation is rearranged there results

$$\sigma_{\omega t} = \varepsilon_a E_1 \left[\frac{(\omega\tau)^2}{1+(\omega\tau)^2} \sin \omega t + \frac{\omega\tau \cos \omega t}{1+(\omega\tau)^2} \frac{\omega\tau}{1+(\omega\tau)^2} e^{-\frac{t}{\tau}} \right] + \varepsilon_a E_2 \sin \omega t$$

and

$$\sigma_{\omega t} = \varepsilon_a \sin \omega t \left[E_1 \frac{(\omega\tau)^2}{1+(\omega\tau)^2} + E_2 \right] +$$

$$+ \varepsilon_a \cos \omega t \left[E_1 \frac{\omega\tau}{1+(\omega\tau)^2} \right] - \qquad (6)$$

$$- \varepsilon_a e^{-\frac{t}{\tau}} \left[E_1 \frac{\omega\tau}{1+(\omega\tau)^2} \right]$$

With a sinusoidal deformation of the three-parameter-model, we get a proportion of stress which likewise changes sinusoidally and runs in phase with the deformation. The second component changes cosinusoidally, i.e. proportional to the deformation speed. The third term represents a damping function which for t tends toward infinity becomes zero.

Equation (6) may therefore be considered a transient response of a sine wave. In steady-state oscillation the following is valid for the stress

$$\sigma_{\omega t} = \varepsilon_a \sin \omega t \left[E_1 \frac{(\omega\tau)^2}{1+(\omega\tau)^2} + E_2 \right] + \varepsilon_a \cos \omega t \left[E_1 \frac{\omega\tau}{1+(\omega\tau)^2} \right] \qquad (7)$$

The proportion of the E-modulus which runs in phase with the deformation, is defined as dynamic E-modulus E'.

$$E' = E_1 \frac{(\omega\tau)^2}{1+(\omega\tau)^2} + E_2 \qquad (8)$$

That proportion of the E-modulus that is effective in phase with the deformation speed, is termed loss modulus.

$$E'' = E_1 \frac{\omega\tau}{1 + (\omega\tau)^2} \qquad (9)$$

In resonating condition the following is true for the three-parameter-model during sinusoidal deformation

$$\sigma_{\omega t} = \varepsilon_a (E' \sin\omega t + E'' \cos \omega t) \qquad (10)$$

If the visco-elastic properties E' and E'' are entered in equation (6), then the following is valid for the stress during the transient

$$\sigma_{\omega t} = \varepsilon_a \left(E' \sin\omega t + E'' \cos \omega t - E'' e^{-\frac{t}{\tau}}\right) \qquad (11)$$

The damping element also contains the relaxation time τ In order to be able to express τ by visco-elastic magnitudes, their dependency on the angular velocity has to be considered, since for the three elements of model E_1, E_2 and η only two defining equations are available. If equations (8) and (9) are combined the following is true

$$E' = E_2 + E_1 - \frac{E''}{\omega\tau}$$

or

$$E' = E_2 + E''\omega\tau$$

and for the derivatives according to $d\omega$

$$(E')' = -\frac{1}{\tau}\left[\frac{\omega (E'')' - E''}{\omega^2}\right]$$

or

$$(E')' = +\tau \left[\omega (E'')' + E'' \right]$$

Both derivatives are equated

$$\frac{1}{\tau} = \omega \sqrt{\frac{E'' + \omega (E'')'}{E'' - \omega (E'')'}}$$

The damping element is written by the formula

$$-\varepsilon_a E'' e^{-\omega t \sqrt{\frac{E'' + \omega (E'')'}{E'' - \omega (E'')'}}}$$

The following function results for the stress at the position ωt

$$\sigma_{\omega t} = \varepsilon_a \left[E' \sin \omega t + E'' \cos \omega t - E'' e^{-\omega t \sqrt{\frac{E'' + \omega (E'')'}{E'' - \omega (E'')'}}} \right] \quad (12)$$

The stress which results from a sinusoidal deformation of the visco-elastic model may be computed if the visco-elastic data in steady-state oscillation and the change of the data in respect to the angular velocity are known. Since the visco-elastic properties in their dependency on the angular velocity within a certain frequency range may always be described by a power function in first approximation, the following is valid

$$E'' = C \omega^x$$

x = exponent of the power function
C = constant factor

The derivative according to dω results in

$$(E'')' = C \times \omega^{x-1} = C \times \frac{1}{\omega}\,\omega^{x} = \frac{x}{\omega}\,E''$$

Thus we get the following for the root term of the damping element

$$\sqrt{\frac{E'' + \omega\,(E'')'}{E'' - \omega\,(E'')'}} = \sqrt{\frac{E'' + x\,E''}{E'' - x\,E''}} = \sqrt{\frac{1+x}{1-x}} \qquad (13)$$

Accordingly, for the stress the following is valid

$$\sigma_{\omega t} = \varepsilon_a \left[E' \sin \omega t + E'' \cos \omega t - E'' e^{-\omega t \sqrt{\frac{1+x}{1-x}}} \right] \qquad (14)$$

If we write

$$\sqrt{\frac{1+x}{1-x}} = z$$

then there results

$$\sigma_{\omega t} = \varepsilon_a \left(E' \sin \omega t + E'' \cos \omega t - E'' e^{-\omega t z} \right) \qquad (15)$$

Herewith we may compute the stress which results from a sinusoidally changing strain, if at the time $t = 0$ $\sigma\omega t = 0$ and $\varepsilon\omega t = 0$.

The deduction of equation (15) was executed with the aid of a three-parameter-model. The restriction to the approximation of the semi-circular strain distribution by a sinusoidal one, allowed us to substitute for the elements of the model ($E_1 : E_2 : \eta$) the visco-elastic properties, which are derived during dynamic sinusoidal pressure change deformation on the test stand. The roller covers as visco-elastic materials are, of course, not as simple in construction. In order

to reproduce their behaviour in dependency on the deformation frequency over the entire frequency range, we would require a model made up of an infinite number of springs and dampers. For every one of the test points, i.e. for E' and E'' with a certain frequency, a simple mechanical model can reproduce the behaviour during sinusoidal stress with the same frequency. If, moreover, the change of the visco-elastic properties at this frequency is known, then the three-parameter model may be so construed that the transient phenomenon may also be determined.

For the analysis of equation (15) we introduce the complex E-modulus E^* and $\tan\delta$.

$$E' = |E^*|\cos\delta$$

$$E'' = |E^*|\sin\delta$$

$$\tan\delta = \frac{E''}{E'}$$

For $\sigma\omega t$ the following is then valid

$$\sigma_{\omega t} = \varepsilon_a E^* (\sin\omega t \cos\delta + \cos\omega t \sin\delta - \sin\delta \; e^{-\omega t z})$$

$$\sigma_{\omega t} = \varepsilon_a E^* \left[\sin(\omega t + \delta) - \sin\delta \; e^{-\omega t z}\right] \qquad (16)$$

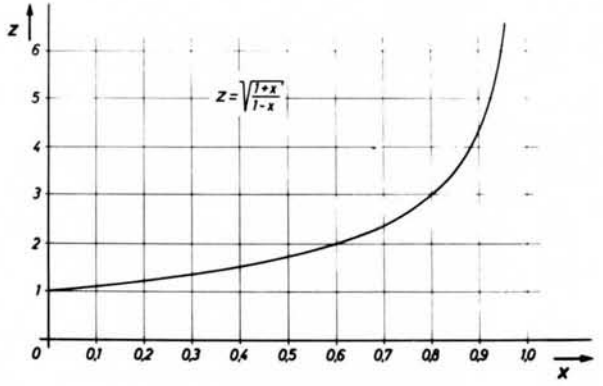

Ill.12: The influence of the exponent x of the function $E''C = \omega^x$ on z.

In order to be able to estimate the influence of z, we entered z as function of x in Illustration 12. For the cover materials examined in the Institute, z ranged between 1,0 and 1,73. The larger z was, the faster the damping element approached zero.

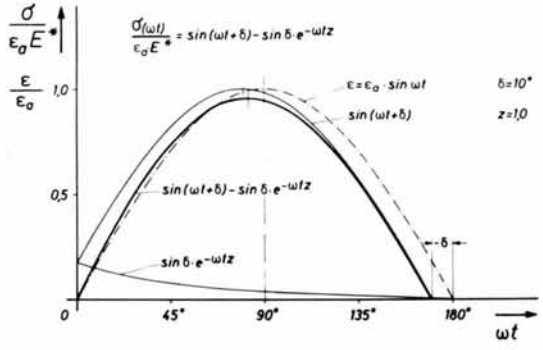

Ill. 13: Stress distribution for $\delta = 10^{\circ}$.

In illustration 13 the stress

$$\varepsilon_{\omega t} = \varepsilon_a \sin \omega t$$

was first entered from $\omega t = 0$ to $\omega t = \pi$

In steady-state oscillation the following is valid for the stress

$$\sigma_{\omega t} = \varepsilon_a E^* \sin(\omega t + \delta)$$

If the deformation starts at the time $t = 0$ with $\varepsilon = 0$ and $\sigma = 0$, then the damping element

$$(= -\sin \delta \; e^{-\omega t z})$$

must be considered.

The solid curve reproduces the stress curve in accordance with equation (16).

The influence of the damping element affects mostly the start of the deformation; at the end of the first half cycle of the sine wave its influence has almost completely worn off. The

stress curve of the transient there coincides substantially with the stress curve of the steady-state.

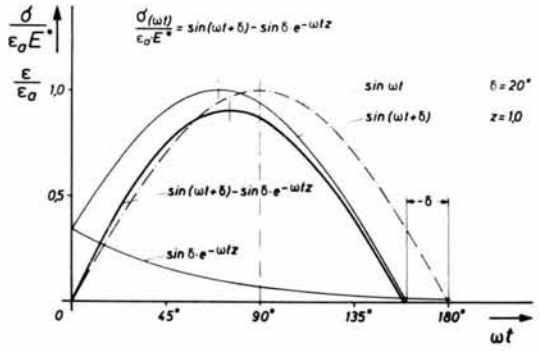

Ill. 14: Strain distribution for $\delta = 20^{\circ}$.

In Illustration 14 the phase angle δ was increased to 20 degrees. Here too, the transient is largely replaced by the steady-state behaviour. The nip width is determined by δ.

The **stress** maximum shifts even further toward the entry **side**. The maximum value of the stress is lower **than in** illustration 13 since the damping element because of $\sin\delta$ moves slower towards zero.

The exact zero position determination results from equating zero of the equation (16)

$$\sin(\omega t + \delta) = \sin\delta\ e^{-\omega t z}$$

t for $\sigma = 0$, was graphically determined.

The zero position of the transient may be equated with sufficient accuracy with the zero position of the steady-state.

For an understanding of the contraction of the nip width it should be noted that a certain time is required for the recovery of the rubber. A deformed rubber element which is suddenly released, approaches the undeformed condition in accordance with an e-function, that **is** to say that the more

the deformation abates, the slower the recovery takes place. At the discharge end of the nip the speed of recovery of the rubber gets progressively less and the contact between metal roller and rubber roller is lost even before the theoretical nip width is reached. The nip width according to this becomes smaller than with a purely elastic metallic material. The diminution of the nip width is essentially determined by the phase angle δ of the roller material, and is obtained through the sinusoidally changing deformation. Accordingly, we write for the percentile diminution of the nip width

$$\text{Percentile diminution of nip width} = \frac{\delta}{\pi} 100 \ (\%)$$

The maximum impression stress no longer occurs in the center of the nip, instead it is displaced toward the entry area, i.e. in illustration 13 and 14 displaced to the left.

The angle, under which the maximum stress occurs, is obtained by a differentiation of equation (15).

$$\cos(\omega t + \delta) \quad = - z \sin \delta \ e^{-\omega t z}$$

This equation can be solved graphically.

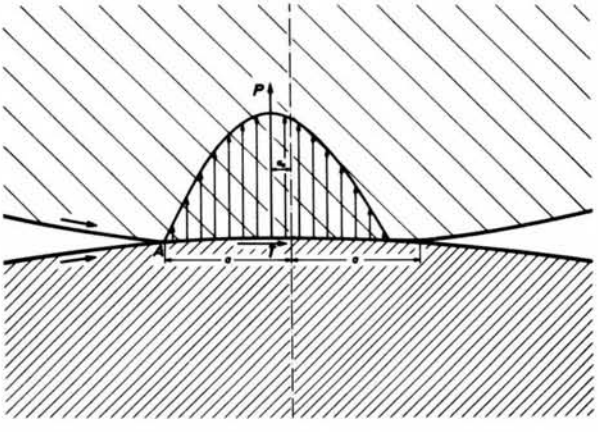

Ill. 15: Pressure distribution in the nip of two rollers

In Illustration 15 the nip of a rigid steel

roller (below) and a visco-elastic roller (above) were depicted. In static condition the width is 2a. By assuming a sinusoidal deformation, we get the stress distribution as shown in illustration 13. The nip width 2a corresponds to $wt \hat{=} 180$ degrees $\hat{=} \pi$. Since the stress distribution in reference to the connection line of the two roller centers becomes asymmetrical, the resulting total force P is displaced by a_o towards the entry side. In order to attain a state of equilibrium which is necessary for maintaining the rolling process, the transmission of a tangential force is required. This tangential force must be transmitted from the steel roller with the radius r to the rubber roller. The product $T \cdot r$ corresponds to the rolling moment which is required for compensation of the visco-elastic losses.

6. Testing Setup for the Study of the Rolling Process of two Rollers.

The theoretical considerations must be confirmed by experiments. For this purpose, a test setup was developed with which the forces between the rollers, the tangential force, the pressure and tangential force distributions in the nip, the width of the nip as well as the slip between the rollers may be measured in a 2-roller system. The following test results are measurements made on four roller combinations of the same geometry but with four different cover materials. The steel roller had a diameter of 100 mm and was driven by an electro-motor with a rate of revolution between 0.5 rps and 20 rps. The diameter of the rubber rollers was 70 mm, the cover thickness 17.5 mm. The visco-elastic data of the four cover materials are identical with those reproduced in illustration 9 and 10.

Of the test equipment we shall show only a two-component receiver for the simultaneous determination of the pressure and tangential forces.

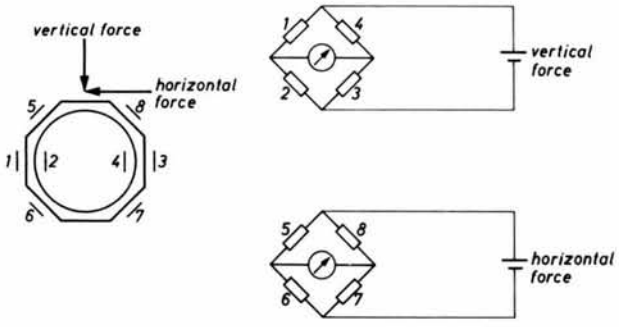

Ill.: 16: Two Component pick-up for the simultaneous Determination of the vertical and horizontal Forces.

The strain gauges 1, 2, 3 and 4 respond only to the vertical forces, the strain gauges 5, 6, 7 and 8 pickup only the tangential forces. This receiver was used for the determination of the contact pressure and the tangential force as well as for the determination of the pressure distribution and the tangential force distribution in the nip.

7. The Pressure Distribution in the Nip of two Rollers.

The four roller covers which were tested have an E-modulus that varies greatly: for three of the cover materials the loss factor is similar, the fourth cover material (Artex) on the other hand has double the loss factor.

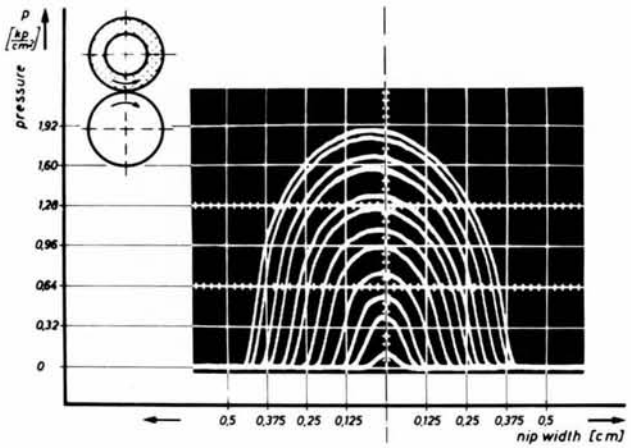

Ill.: 17: Pressure Distribution Curves in different Settings for the Cover Material 154 N

In Illustration 17 the pressure distribution curves for settings 0.1 mm to 1 mm were reproduced. The pressure distribution curves all show the characteristic features based on theoretical considerations. Half of the nip width on the entry side is larger than on the exit side. The maximum pressure is shifted toward the entry side. With a roller cover material that has a larger or smaller E-modulus but the same loss factor, only the maximum pressure changes, the course of the curve, however, remains approximately the same.

In Illustration 18 the pressure distribution curves for the cover material Artex were reproduced. This cover material has double the loss factor than the cover material 154 N of the last illustration. Accordingly, the nip width has decreased and the pressure maximum has shifted even more to the entry side.

This measuring data shows clearly that the influence of the visco-elastic characteristic values on the pressure distribution in the nip is qualitatively accurately reproduced by mathematical theory.

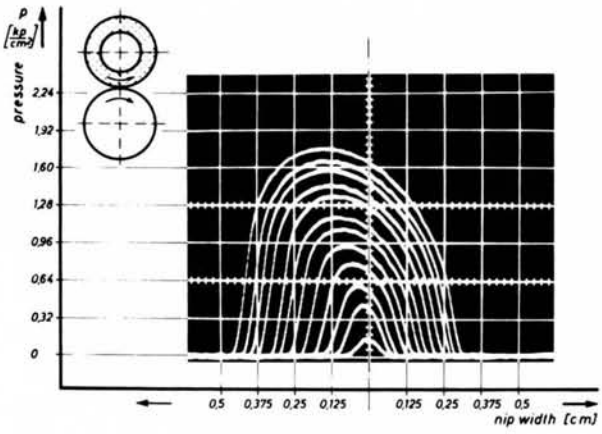

Ill.: 18: Pressure Distribution Curves at various Setting for the Material Artex.

8. The Dependency of the Contact Pressure on the Rate of Revolution.

Hitherto, only the course of the pressure distribution in the nip was determined theoretically. By integration of this pressure distribution curve the total force is determined, with which the rollers are pressed against each other. If the length of the rollers is designated as l and the width of the nip of a material without loss factor as 2a, then we get

$$P = l\frac{2a}{\pi}\int_0^{\pi-\delta} \sigma_{\omega t}\, d\omega t$$

From this it follows that

$$P = \varepsilon_a E^* l\frac{2a}{\pi}\int_0^{\pi-\delta}\left[\sin(\omega t+\delta) - \sin\delta\; e^{-\omega t z}\right] d\omega t$$

The force P shows itself as a function of the complex E-modulus and of the phase angle δ. If the adjustment of two rollers is kept constant and the rate of revolution is changed, then the force P will likewise change, since the E-modulus as well as the loss angle change with the deformation frequency. With the four cover materials that were used for this rolling test, the phase

angle changes by about 3 degrees between 1 Hz and 100 Hz. An analysis of the equation shows that with a change of the phase angle by these 3 degrees, the force changes by 2 percent. Since the change of the complex modulus is by far greater, it determines the rate of revolution dependency of the force and we write

$$P \sim E^*$$

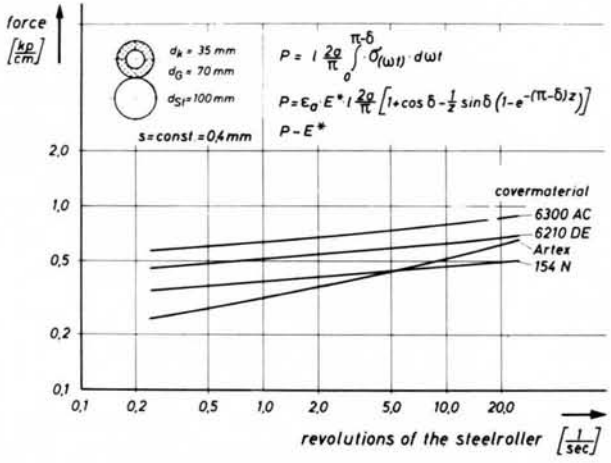

Ill. 19: Forces between the Rollers in Dependency on the Rate of Revolution for four Cover Materials.

In Illustration 19 the forces that act between the two rollers at a constant adjustment of 0.4 mm were plotted in dependency on the number of revolutions for four roller combinations. The force gradient as function of the rate of revolutions occurs analogously to the gradient of the complex E-modulus with an increase of the deformation frequency in illustration 9.

9. The Dependency of the Tangential Force on the Rate of Revolutions.

A transmission (transfer) of a tangential force in the nip is required to compensate the viscoelastic losses which occur in the cover materials during rolling. For the rolling moment we get

in non-dimensional notation

$$\frac{M}{E^* \varepsilon_a \, l} \cdot \frac{\pi^2}{4a^2} = \frac{\pi}{2}\left[1+\cos\delta - \frac{1}{z}\sin\delta\left(1-e^{-(\pi-\delta)z}\right)\right] -$$

$$-\left\{\pi-\delta-\sin\delta - \sin\delta\,\frac{1}{z}\left[\frac{1}{z}-\left(\frac{1}{z}+\pi-\delta\right)e^{-(\pi-\delta)z}\right]\right\}$$

The right side of the equation encompasses the influence of the phase angle. If the adjustment (setting) of the rollers is kept constant, then the following is valid

$$M = T \cdot r \quad E^* \cdot f(\delta)$$

For the cover material 154 N the following is valid as the function of the frequency for the complex E-modulus

$$E^* = E_1^* \left(\frac{f}{f_1}\right)^{0,085}$$

and for the loss factor

$$\tan\delta = \tan\delta_1 \left(\frac{f}{f_1}\right)^{0,1}$$

For these material values the rolling moment was calculated and depicted in Illustration 20.

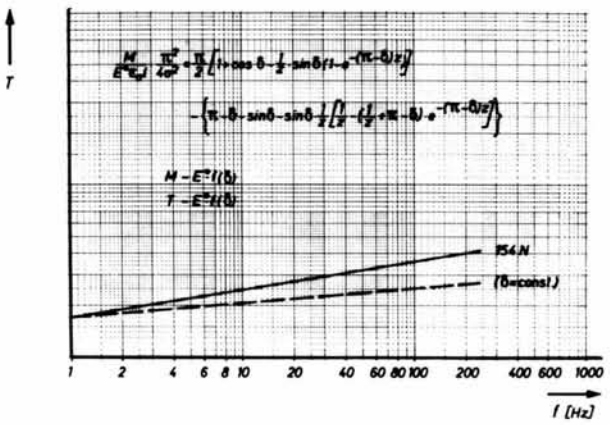

Ill. 20: Rolling Moment for Material 154 N as a Function of Frequency.

With increasing deformation frequency, the rolling moment increases greatly. To clarify the significance of the loss factor, the rolling moment, which at constant loss factor would result only on the basis of the change of the E-modulus, was marked by a dotted line. It is very evident that the loss factor is an essential magnitude.

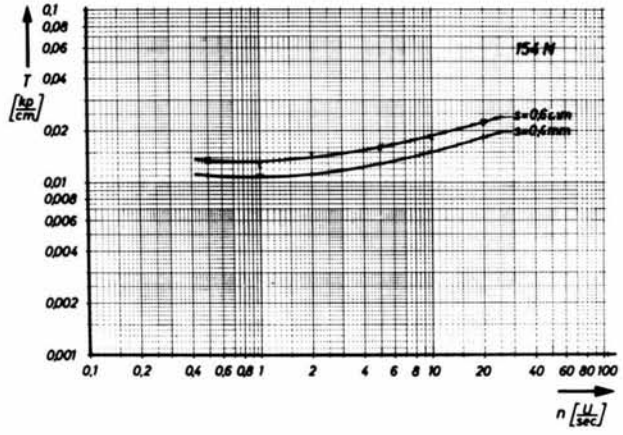

Ill. 21: Experimentally determined tangential Forces of a Roller Combination with Material 154 N.

In Illustration 21 the measured tangential forces as a function of frequency for a roller combination with the same cover material 154 N were depicted. The slopes of the curves are not quite in agreement with our theoretical curve. This is a problem of measuring the tangential forces because the friction in the bearings is also contained in the results.

Final Comments:

The deliberations and experimental results quoted in this report were meant to show the significance of the visco-elastic behaviour of cover materials in the rolling process. On the oner hand, a test setup was described which permits the determination of the visco-elastic characteristic values of pressure and ink rollers and on the other hand, we have a simple theoretical consideration, which enables us to determine the influence of the measured material magnitudes on the rolling process.

The rolling processes occurring in printing presses are far more complicated than the simple rolling system examined here. The influence of the ink, the paper and the forme makes the rolling process even more complex. I do believe, however, that for a discussion of the special printing engineerical influences, the understanding of the cover material influence is of great advantage.

The aforementioned research is financed by The Research Association for Printing Machines together with allocations from the Federal Ministry of Commerce through the Industrial Research Associations (AIF).

Selected Bibliography

Ecker, R.:
1953.a Dynamische Dämpfung und E-Modul im kautschuk-elastischen Bereich, Kautschuk und Gummi, 6, Nr. 7, S. 127-139 WT.

Ecker, R.:
1956.b Temperaturabhängigkeit statischer und dynamischer Verformungseigenschaften von Kautschuk-Vulkanisaten und anderen Hochpolymeren, Kautschuk und Gummi, 9, Nr. 1, S. 14-17 WT.

Eschenbach, W. und Pfeiffer, G.:
1965 Werkstoffeigenschaften von Presseurbelägen, Zwischenbericht zur Sitzung des Technischen Ausschusses der Forschungsgesellschaft Druckmaschinen e.V., S. 17-28, Darmstadt.

Evans, I.: The rolling resistance of a wheel
1954 with a solid rubber tyre. Brit.J. Appl. Phys. vol. 5, pp.187-88.

Ferry, J.: Viscoelastic Properties of Polymers, John Wiley & Sons, New York-London.
1961

Flom, D.G.: Rolling Friction of Polymeric
1961 Materials, J. Appl. Phys. vol.32, No. 8, Aug. 1961, pp.1426-1436.

Funk, G.: Triebkraft und Drehmoment bei
1938 Hochdruck-Rotationsmaschinen. Ein Beitrag zur Theorie des Rollwiderstandes an Walzenpaaren. Diss. Deutsche Zentraldruckerei, Berlin SW 11.

Hunter, S.C.:
1961 The Rolling Contact of a Rigid Cylinder with a Viscoelastic Half Space. J. Appl. Mech. 28, pp. 611-617.

May, W.D., Morris, E.L., and Atack, D.:
1959 Rolling Friction of a Hard Cylinder over a Viscoelastic Material. J. Appl. Phys. vol.30, pp.1713-24.

Contd. Selected Bibliography

Morland, L.W.:
1962 a A Plane Problem of Rolling Contact in Linear Viscoelasticity Theory. J. Appl. Mech. vol.28, 345-352.

Morland, L.W.:
1967 b Exact Solutions for Rolling Contact between Viscoelastic Cylinders. Quart.Journ.Mech. and Appl. Math., vol. XX, Pt. 1.

Nitsche, R. und Wolf, K.:
1962 Kunststoffe, Band 1 und 2, Springer-Verlag, Berlin-Göttingen-Heidelberg.

Oberst, H.:
1963 Elastische und viskose Eigenschaften von Werkstoffen, Grundlagen und Begriffe, Beuth-Vertrieb GmbH., Berlin-Köln-Frankfurt.

Stuart, H.A.:
1956 Die Physik der Hochpolymeren, Band 4, Springer-Verlag, Berlin-Göttingen-Heidelberg.

Tabor, T.:
1952 The Mechanism of Rolling Friction. Phil. Mag., 43, p. 1055-1059,1952

Tabor, T.: Elastic Work involved in rolling
1955 a sphere on another surface. Brit. J. Appl. Phys. 6, 79, 1955

Cook, N.H., Loewen, E.G., Shaw, M.C.:
1954 Machine-Tool Dynamometers. American Machinist 98 (1954) pp.125 - 129